Improved Atomic Norm Based Time-Varying Multipath Channel Estimation

Jianxiu Li, *Graduate Student Member, IEEE*, and Urbashi Mitra, *Fellow, IEEE*

***Abstract*— In this paper, improved channel gain delay estimation strategies are investigated when practical pulse shapes with finite block length and transmission bandwidth are employed. Pilot-aided channel estimation with an augmented atomic norm based approach is proposed to promote the low rank structure of the time-varying narrowband leaked channel. All the channel parameters, *i.e.*, delays, Doppler shifts, and channel gains are recovered. Design choices which ensure unique estimates of channel parameters for rectangular, Gaussian, and root-raised-cosine pulse shapes are examined in the noiseless case, respectively. Furthermore, a perturbation analysis is conducted to measure the impact of noise and further design choices for parameters are proposed to mitigate the effects of noise. Finally, numerical results verify the theoretical analysis and show performance improvements over the previously proposed method.**

***Index Terms*— Atomic norm, low-rank, re-sampling, channel estimation, time-varying narrowband leaked channel.**

I. Introduction

MANY wireless communication applications necessitate high performance channel estimation in order to ensure reliable communications. In particular, frequency and temporal distortion [2] are a challenge in high mobility scenarios, such as high-speed railway systems [3], vehicle-to-vehicle communications [4], positioning systems [5], and unmanned aerial vehicle-assisted networks [6].

To combat channel distortion, equalization with accurate channel estimation has been persistently studied (see *e.g.* [7]–[11]). Inherent channel sparsity has been exploited in [9]–[11], reducing the number of observations needed for estimation; however, these works ignore the impact of practical pulse shapes which lead to a loss in sparsity (channel leakage) in the Doppler-delay domain and challenge performance of these sparse methods.

Manuscript received January 8, 2021; revised May 3, 2021; accepted May 30, 2021. Date of publication June 9, 2021; date of current version September 16, 2021. This work has been funded in part by one or more of the following: Cisco Foundation 1980393, ONR N00014-15-1-2550, ONR 503400-78050, NSF CCF-1410009, NSF CCF-1817200, NSF CCF-2008927, Swedish Research Council 2018-04359, ARO W911NF1910269, and DOE DE-SC0021417. This article was presented in part at the IEEE International Conference on Acoustics, Speech and Signal Processing (ICASSP 2021) [1]. The associate editor coordinating the review of this article and approving it for publication was Y. Wu. *(Corresponding author: Jianxiu Li.)*

The authors are with the Department of Electrical and Computer Engineering, University of Southern California, Los Angeles, CA 90089 USA (e-mail: jianxiul@usc.edu; ubli@usc.edu).

Color versions of one or more figures in this article are available at https://doi.org/10.1109/TCOMM.2021.3087793.

Digital Object Identifier 10.1109/TCOMM.2021.3087793

Channel leakage has been addressed by enhancing classical sparse approximation [4], [12], [13]. Another promising way is to adopt alternative representations of the wireless channel. Basis expansion models (BEM), modeling the time-varying channels as a weighted summation of a few basis functions, is investigated in [14], [15]. Different from the basis expansion in [12], these basis functions for BEM are fixed and known to the receiver. Therefore, only a few BEM coefficients need to be estimated as compared with the unknown channel parameters [15], resulting in a reduction in the number of pilot symbols. However, individual channel parameters are not available from the estimated BEM coefficients and the model error of BEM may severely degrade the estimation accuracy when the BEM based approaches are applied to practical communication systems.

Distinct from the prior works, [16] exploits the atomic norm heuristic [17], [18] to promote structure, while explicitly considering the leakage. In this work, the single-carrier signals transmitted over the linear, time-varying and narrowband leaked channel exhibit a parametric, low rank, bilinear form. By exploiting the inherent structure, the parametric low-rank atomic norm approach (PLAN) in [16] outperforms [4], [12] in terms of the estimation accuracy and bit error rate (BER) of data sequences. The extensions of [16] to the orthogonal frequency-division multiplexing leaked channel are presented in [20]–[22]; however, only the channel matrix is estimated in these works [16], [20]–[22]. Even though the approach of explicitly recovering Doppler shifts is also presented in [16], delays and channel gains are not separately recovered. In contrast to the equalization achieved only with the estimated channel matrix, improved equalization is enabled via the direct estimation of channel gains and delays. In addition, based on the estimated delays and channel gains, time-of-arrival or received signal-strength information can be exploited for localization [23]–[26], which is critical to many internet-of-things applications.

In this paper, we further improve upon the atomic norm based approach for single-carrier systems. Herein, we augment the method of [16] and employ the estimated Doppler and channel leakage vectors to further resolve channel gains and the delays by exploiting knowledge of the pulse shape. Explicit channel state information (CSI) in the form of Doppler shifts, path delays and channel gains enables the construction of a channel and pulse matched filter. Furthermore, with such CSI, re-sampling and re-estimation of all parameters with

further improved quality is achievable. We observe that modest improvements on the estimation accuracy can lead to significant improvements of the BER as seen in [27].

The main contributions of this paper are:

1) An enhancement to the atomic norm based channel estimation scheme [16] is proposed, where the delay, Doppler shift, and channel gain of each path can be individually estimated, in contrast to [16].
2) The conditions for unique delay estimates for rectangular, Gaussian, and root-raised-cosine (RRC) pulse shapes are provided for the noiseless case.
3) A perturbation analysis for the noisy scenario is investigated. The analysis suggests the appropriate values of key design parameters to optimize performance.
4) The theoretical analyses for uniqueness and perturbation are validated via simulation.
5) The BER of data sequences and the normalized mean-squared error (NMSE) for the channel matrix and Doppler shifts of the new scheme are compared to that for [16]; strong gains in performance are seen despite the simplicity of the proposed scheme.

Our prior work [1] introduced the improved atomic norm based channel estimator and discussed the parameters design specific to the RRC pulse shapes. Herein, we complete our scheme and present a systematic approach for the pulse-shape based parameter design. Furthermore, analysis regarding the uniqueness of delay estimate for the rectangular pulse shape and Gaussian pulse shapes is provided. In order to assess robustness to noise, we provide a perturbation analysis of the algorithm and further derive proper parameter values to maximize robustness. The uniqueness and perturbation analyses are provided for the three different pulse shapes. Full derivations and proofs are provided herein in contrast to [1].

The rest of this paper is organized as follows. Section II introduces the signal model of the time-varying narrowband leaked channel. Section III presents the design of the improved atomic norm based channel estimation. Then, in Section IV, the proposed scheme with three typical pulse shapes is theoretically analyzed, where the uniqueness of the delay estimate is ensured in the noiseless case. In addition, a perturbation analysis is provided to further analyze accurate estimation via the proper choices of design parameters. The numerical results are given in Section V to verify the theoretical analysis and show the performance improvements. Finally, the paper is concluded in Section VI. Appendices, A, B, and C provide the proofs of the propositions and lemma of this work.

Notation: Scalars are denoted by lower-case letters, x and column vectors by bold letters, $\boldsymbol{x}$. The ith element of x is denoted by $x[i]$. A matrix is denoted by bold capital letters, $\boldsymbol{X}$, and its $(i,\ j)$th element by $X[i,j]$. The operators $\lfloor x \rfloor$, $|x|$, $< x >$, $\|\boldsymbol{x}\|_2$, $\text{sign}(x)$ and $\max(\mathcal{A})$ represent the largest integer that is less than x, the magnitude of x, the integer that is closest to x, the ℓ_2 norm of $\boldsymbol{x}$, the sign of x and the maximum value in set $\mathcal{A}$, respectively. The notation $\otimes$ denotes the convolution. The operators $\text{trace}(\cdot)$, $(\cdot)^T$, and $(\cdot)^H$ are defined as the trace of a matrix, the transpose of a matrix or vector, and the conjugate transpose of a vector or matrix, respectively.

II. Signal Model

We adopt the signal model of [16], thus, the transmitted signal $x(t)$ is given by

$$x(t) = \sum_{n=-\infty}^{+\infty} x[n] p_t\left(t - nT_s\right), \tag{1}$$

where $p_t(t)$, T_s, and $x[n]$ represent the transmit pulse, the sampling period, and the pilot sequence, respectively. Since the signal is transmitted over a linear, time-varying and narrowband channel whose impulse response is given by

$$g(t,\tau) = \sum_{k=1}^{p_0} \eta_k \delta\left(\tau - t_k\right) e^{j2\pi\nu_k t}, \tag{2}$$

the received signal can be written as

$$y(t) = \int_{-\infty}^{+\infty} g(t,\tau) x(t-\tau) d\tau + z(t), \tag{3}$$

where $z(t)$ is a complex, Gaussian, white noise process, p_0 denotes the number of dominant paths, η_k, v_k, and t_k represent the channel gain, Doppler shift, and delay of the kth path, respectively, with $1 \le k \le p_0$. We label the paths according to the delay values, thus the first path has the smallest delay value t_1. At the receiver, the received signal is converted to the discrete-time equivalent by matched filtering with $p_r(t)$, that is, $y(t) \otimes p_r(t)$, and then sampled at $t = nT_s + t^\star(n)$, where the offset, $t^\star(n)$, is a design parameter. Hence, the corresponding discrete-time signal is given by

$$\begin{aligned} y[n] &= \left(x(t) \otimes g(t,\tau) \otimes p_r(t) + z(t) \otimes p_r(t)\right)|_{t=nT_s+t^\star(n)} \\ &= \sum_{m=0}^{M-1} \sum_{k=1}^{p_0} \eta_k e^{j2\pi v_k[(n-m)T_s+t_k]} p\left(mT_s + t^\star(n) - t_k\right) \\ &\quad \times x[n-m] + z[n], \end{aligned} \tag{4}$$

where $p(t) = p_t(t) \otimes p_r(t)$, $z[n] = z(t) \otimes p_r(t)\,|_{t=nT_s+t^\star(n)}$, $0 < m < M = \left\lfloor \frac{\tau_{\max}}{T_s} \right\rfloor + 1$, $M \le n < N + M - 1$, $\tau_{\max} = \max(t_1, \ldots, t_{p_0})$, and N denotes the length of the pilot sequence. We refer readers to [4] for more details of this signal model.

If $t^\star(n) = 0$ for each n, the received discrete-time signal is

$$\begin{aligned} y[n] &= \left(x(t) \otimes g(t,\tau) \otimes p_r(t) + z(t) \otimes p_r(t)\right)|_{t=nT_s} \\ &= \sum_{m=0}^{M-1} \sum_{k=1}^{p_0} \eta_k e^{j2\pi v_k((n-m)T_s+t_k)} p\left(mT_s - t_k\right) \\ &\quad \times x[n-m] + z[n]. \end{aligned} \tag{5}$$

Note that, we assume $p_t(t) = p_r(t)$. The receiver knows the pilot sequence as well as the transmit and receive pulse shapes. We seek to estimate the channel parameters, (η_k, v_k, and t_k for $1 \le k \le p_0$), given the number of dominant paths.

III. Improved Atomic Norm Based Channel Estimation

A. Estimation Strategy

Prior to providing our algorithmic improvements to the methods of [16], we briefly review the estimation strategy

of [16]. Defining $\bar{v}_k = v_k T_s$, $l_k(t) = p(t-t_k)e^{-j2\pi v_k t}$, $\boldsymbol{l}_k = \frac{1}{\sum_{m=0}^{M-1} l_k(mT_s)} \left[l_k(0T_s), \cdots, l_k((M-1)T_s)\right]^T$, and $\boldsymbol{\alpha}(\bar{v}) = \left[e^{-j2\pi M\bar{v}} \quad \cdots \quad e^{-j2\pi(N+M-1)\bar{v}}\right]^T$, the received discrete-time signal in Equation (5) can be rewritten as

$$\begin{aligned} y[n] &= \sum_{k=1}^{p_0} \bar{\eta}_k \boldsymbol{\alpha}\left(\bar{v}_k\right)^H \boldsymbol{c}_{n-M+1} \boldsymbol{x}_n^T \boldsymbol{l}_k + z[n] \\ &= \operatorname{trace}\left(\boldsymbol{c}_{n-M+1}\boldsymbol{x}_n^T \sum_{k=1}^{p_0} \bar{\eta}_k \boldsymbol{l}_k \boldsymbol{\alpha}\left(\bar{v}_k\right)^H\right) + z[n], \end{aligned} \tag{6}$$

where $\boldsymbol{x}_n = [x[n], \cdots, x[n-(M-1)]]^T$, $\bar{\eta}_k = \eta_k e^{j2\pi v_k t_k} \sum_{m=0}^{M-1} l_k(mT_s)$, $\bar{v}_k \in [-\frac{1}{2}, \frac{1}{2}]$, and $\boldsymbol{c}_n$ is a vector of length N, with the n-th entry being 1 while the others being 0. The channel matrix is a function of the unknown channel parameters:

$$\mathbf{H} = \sum_{k=1}^{p_0} \bar{\eta}_k \boldsymbol{l}_k \boldsymbol{\alpha}\left(\bar{v}_k\right)^H, \tag{7}$$

which establishes a mapping between the transmitted discrete-time signals and the received discrete-time signals in the absence of noise. Given that many channels of interest have a small number of paths relative to the number of observations $p_0 \ll N$, we can formulate a parametric low-rank matrix recovery problem. Stacking $y[n]$ for $M < n < N+M-1$ in a vector $\boldsymbol{y}$, we can write

$$\boldsymbol{y} = \Pi\left(\mathbf{H}\right) + \boldsymbol{z}, \tag{8}$$

where $\boldsymbol{z} = [z[M], \cdots, z[N+M-1]]^T$, and the linear operator $\Pi : \mathbb{C}^{M\times N} \rightarrow \mathbb{C}^{N\times 1}$ is defined as $\Pi\left(\mathbf{H}\right)[n] = \operatorname{trace}\left(\boldsymbol{c}_{n-M+1}\boldsymbol{x}_n^T\mathbf{H}\right)$. Since each term in the sum in Equation (7) is a rank-one matrix, [16] proposes the use of the atomic norm [17], [18] to promote sparsity. Given a set of atoms, $\mathcal{A} = \left\{e^{j\theta}\boldsymbol{l}\boldsymbol{\alpha}(\bar{v})^H : \bar{v} \in [-\frac{1}{2}, \frac{1}{2}], \|\boldsymbol{l}\|_2 = 1, \boldsymbol{l} \in \mathbb{C}^{M\times 1}, \theta \in [0, 2\pi)\right\}$, the atomic norm is defined as

$$\begin{aligned} \|\mathbf{H}\|_{\mathcal{A}} &= \inf\left\{c > 0 : \mathbf{H} \in c\,\mathrm{conv}(\mathcal{A})\right\} \\ &= \inf_{\bar{\eta}_k, \bar{v}_k, \|\boldsymbol{l}_k\|_2 = 1} \left\{\sum_k |\bar{\eta}_k| : \mathbf{H} = \sum_k \bar{\eta}_k \boldsymbol{l}_k \boldsymbol{\alpha}\left(\bar{v}_k\right)^H\right\}, \end{aligned} \tag{9}$$

where $\mathrm{conv}(\mathcal{A})$ is the convex hull of $\mathcal{A}$. Using the atomic norm, we solve the following optimization problem to estimate the channel [16], [19],

$$\underset{\mathbf{H}}{\text{minimize}} \|\mathbf{H}\|_{\mathcal{A}} \text{ s.t. } \|\boldsymbol{y} - \Pi(\mathbf{H})\|_2 \leq \epsilon, \tag{10}$$

where ϵ is a bound on $\|\boldsymbol{z}\|_2$, *i.e.*, $\|\boldsymbol{z}\|_2 \leq \epsilon$. In [18], our optimization problem in Equation (10) is shown to have an equivalent semi-definite program representation, which enables efficient solution of Equation (10) via solvers such as CVX [28]. Under key conditions (C-1 and C-2 of [16]), the Doppler shifts can be estimated by finding the roots of the following equation:

$$\Lambda(\bar{v}) = 1 - \left\| \left(\sum_{n=1}^{N} \boldsymbol{\lambda}[n] \boldsymbol{x}_n \boldsymbol{c}_{n-M+1}^T\right) \boldsymbol{\alpha}(\bar{v}) \right\|_2, \tag{11}$$

where $\boldsymbol{\lambda}$ is the optimal solution of the dual problem corresponding to the primal optimization problem in Equation (10). A key result of [16] is that the solution of the optimization problem in Equation (10) is the optimal and unique solution of the channel estimation problem if $\boldsymbol{z} = \mathbf{0}$. We refer readers to [16] for the details of the atomic norm based Doppler shift estimation. This concludes the summary of prior work.

We next present the augmented scheme which provides the estimates of the delays and the channel gains, building on the estimates of [16]. In Equation (5), we replace the Doppler shifts v_k by their estimated values, $\hat{v}_k$ for $1 \leq k \leq p_0$, to construct an estimate of the channel leakage vector, $\hat{\boldsymbol{h}}_{\boldsymbol{m}}^{\boldsymbol{l}}$. We assume that the estimates are perturbed from the true values as follows

$$\hat{\boldsymbol{h}}_m^l = \boldsymbol{h}_m^l + \boldsymbol{e}_m^{(h)}, \tag{12}$$

where the kth element of the true channel leakage vector $\boldsymbol{h}_m^l$ with $0 \leq m \leq M-1$, is given by

$$\boldsymbol{h}_m^l[k] = \eta_k e^{j2\pi v_k(t_k - mT_s)} p\left(mT_s - t_k\right), \tag{13}$$

for $1 \leq k \leq p_0$. The vector $\boldsymbol{e}_m^{(h)}$ represents the error induced by the errors in the estimation of the Doppler shifts. From Equations (6) and (13), we can see that the channel delays appear only in the channel leakage vector. How to obtain the estimated delays and channel gains based on the estimated channel leakage vector $\hat{\boldsymbol{h}}_m^l$, $0 \leq m \leq M-1$, is the focus of this section and the main contribution of this paper.

Since the channel gains are unknown, complex values, we cannot use the phase of $\boldsymbol{h}_m^l$ defined in Equation (13) to directly obtain the delay estimate. However, knowledge of the pulse shape $p(t)$ can be exploited to infer the delays. We define the *ratio function*, which will be used in our estimation strategy, as

$$r_k(t_k) = \frac{p\left(m_2 T_s - t_k\right)}{p\left(m_1 T_s - t_k\right)} + e^{(r_k)}, \tag{14}$$

with $0 \leq m_1, m_2 \leq M-1$ and $m_1, m_2 \in \mathbb{Z}$. Here, the error in the ratio function, $e^{(r_k)}$ is

$$e^{(r_k)} = \operatorname{sign}\left(\frac{p\left(m_2 T_s - t_k\right)}{p\left(m_1 T_s - t_k\right)}\right) \left|\frac{\hat{\boldsymbol{h}}_{m_2}^l[k]}{\hat{\boldsymbol{h}}_{m_1}^l[k]}\right| - \frac{p\left(m_2 T_s - t_k\right)}{p\left(m_1 T_s - t_k\right)}. \tag{15}$$

Note that, if $p(t)$ is positive for all t, we can directly set the ratio function, $r_k(t_k)$ to $\left|\frac{\hat{\boldsymbol{h}}_{\boldsymbol{m_2}}^{\boldsymbol{l}}[k]}{\hat{\boldsymbol{h}}_{\boldsymbol{m_1}}^{\boldsymbol{l}}[k]}\right|$. If $p(t)$ is not positive everywhere, we need to first obtain the sign of $\frac{p(m_2T_s - t_k)}{p(m_1T_s - t_k)}$ and then set $r_k(t_k)$ properly. Algorithm 1 illustrates the generation of these ratios for delay estimation. The reason why we propose to use $r_k(t_k)$ instead of $|r_k(t_k)|$ for delay estimation is to ensure the uniqueness of the delay estimates, which is explained in Section IV. Here, the design parameters m_1 and m_2 are two distinct integers restricted to $[0, M-1]$. Perhaps surprisingly, the choices of m_i strongly influence the uniqueness and quality of the estimates; furthermore, they are pulse-shape dependent. Thus in Section IV, we explore good choices for these parameters for several typical pulse shapes. Once m_1 and m_2 are selected for the kth path, the ratio

Algorithm 1 Ratio Functions for Delay Estimation

Input: $r_k(t_k) = \frac{\hat{\boldsymbol{h}}^l_{m_2}[k]}{\hat{\boldsymbol{h}}^l_{m_1}[k]} = |r_k(t_k)| \times e^{j\phi_{r_k(t_k)}}$ and $\hat{v}_k$, with $1 \le k \le p_0$ and $0 \le m_1, m_2 \le M-1$;
Output: $r_k(t_k)$, with $1 \le k \le p_0$;
for $k = 1$ to p_0 **do**
  $z_k \leftarrow \left\langle \frac{2\pi(m_2-m_1)\hat{v}_k T_s + \phi_{r_k(t_k)}}{\pi} \right\rangle$;
  if $p(t)$ is positive for all t **then**
    $r_k(t_k) \leftarrow |r_k(t_k)|$;
  else
    $r_k(t_k) \leftarrow (-1)^{z_k}|r_k(t_k)|$;
  end if
  $k \leftarrow k+1$;
end for
return $r_k(t_k)$, with $1 \le k \le p_0$.

function is simply a function of t_k, and the delay estimate of the kth path, $\hat{t}_k$, with $1 \le k \le p_0$ can be obtained by

$$\hat{t}_k = (r(t_k))^{-1}. \tag{16}$$

In addition, with good choices of m_1 and m_2, a closed-form expression for $\hat{t}_k$ can be found and the computational complexity of the delay estimation scales as $\mathcal{O}(p_0)$. After the delays are estimated, we can substitute their values into Equation (5) to compute the channel gains, where the Doppler shifts are obtained according to Equation (11). Therefore, all the channel parameters are individually recovered.

B. Re-Sampling

We observe that one can always construct an equalizer from the estimated channel leakage vector and Doppler shifts as in [16]. However, with the estimated delays and channel gains, several applications are enabled such as localization. Furthermore, we can both re-sample the received signal with the proper channel-pulse matched filter as well as re-estimate the channel parameters with the re-sampled signals for more accurate estimation. We note that re-sampling results in a reduction in channel leakage and an increased signal-to-interference-ratio at the receiver. We observe that re-sampling is not possible with PLAN [16].

Specifically, we re-sample the received signal at $nT_s + \hat{t}_{k'}$ with $1 \le k' \le p_0$, and thus have

$$\begin{aligned} y[n] &= \left(x(t) \otimes g(t,\tau) \otimes p_r(t) + z(t) \otimes p_r(t)\right)|_{t=nT_s+\hat{t}_{k'}} \\ &= \sum_{m=0}^{m_0-1} \sum_{k=1}^{p_0} \eta_k e^{j2\pi v_k[(n-m)T_s+t_k]} p\left(mT_s + \hat{t}_{k'} - t_k\right) \\ &\quad \times x[n-m] + z[n]. \end{aligned} \tag{17}$$

Essentially, the receive filter is matched to the pulse shape and the channel with the newly estimated parameters.

The improved estimation strategy is denoted as the Atomic Norm based Delay-Doppler Estimation (ANDE).

IV. Pulse-Shape Based Design Choices

Given that typical pulse-shapes are non-linear with respect to the time argument, the inversion function $r(\cdot)$ needed to compute the delay estimates will also be non-linear. As such, we need further constraints to ensure unique delay estimates. To this end, we show that proper choice of m_1 and m_2 can ensure uniqueness for several common pulse shape functions. In particular, the rectangular, Gaussian, and RRC pulse shapes are investigated, respectively, where we assume $m_2 > m_1$ without loss of generality.

For each pulse shape type, we first view the design parameters m_1 and m_2 as constants and prove that, based on the noiseless ratio function, *i.e.*, $e^{(r_k)} = 0$ for all k, the delays can be efficiently estimated without errors. The analysis herein is for the noiseless case and assumes access to the leakage vector and the Doppler shifts; thus any method can be employed to determine these parameters. Our ANDE strategy exploits the estimated leakage vector and Doppler shifts via PLAN [16], however, the methods for estimating the delays and channel gains can be applied to any strategy providing the needed estimates. Then, a perturbation analysis is conducted to determine how to select the design parameters for the noisy case. We denote the noiseless ratio function by $f(t_k)$ and the perturbation level is defined as $\delta(k) = \frac{e^{(r_k)}}{f(t_k)}$.

A. Rectangular Pulse Shape

The rectangular pulse shape is firstly considered and $p(t)$ is given by

$$p(t) = 1 - \left|\frac{t}{T}\right|, \tag{18}$$

where $2T$ is the support of $p(t)$. For this kind of pulse shape, we assume $2T_s \ll T$ and $MT_s \le T$ hold and thus the bandwidth is essentially determined by the Doppler spread [29]. For fixed m_1 and m_2, the ratio function used to estimate the delay can be expressed as

$$f_R(t_k) = \frac{p\left(m_2T_s - t_k\right)}{p\left(m_1T_s - t_k\right)} = \frac{1 - \left|\frac{m_2T_s - t_k}{T}\right|}{1 - \left|\frac{m_1T_s - t_k}{T}\right|}, \tag{19}$$

for the noiseless case, and correspondingly the delay estimate is given in Equations (20a)-(20c), as shown at the bottom of the page. Therein, we assume that $f_R(t_k) \ne 1$[1] and $f_R(t_k) \ne -1$ because $MT_s \le T$.

Note that the derivation of Equations (20a)-(20c) presumes knowing whether m_iT_s $(i = 1, 2)$ is greater than the true

[1]If $f_R(t_k) = 1$, the delay estimate of the kth path can be directly obtained.

$$\hat{t}_k = \begin{cases} m_1T_s - T + \dfrac{(m_1-m_2)T_s}{f_R(t_k)-1}, & \text{if } m_2T_s \ge t_k \text{ and } m_1T_s \ge t_k; \quad (20a) \\ m_1T_s + T + \dfrac{(m_2-m_1)T_s - 2T}{f_R(t_k)+1}, & \text{if } m_2T_s \ge t_k \text{ and } m_1T_s < t_k; \quad (20b) \\ m_1T_s + T + \dfrac{(m_1-m_2)T_s}{f_R(t_k)-1}, & \text{otherwise} \quad (20c) \end{cases}$$

value of delay. Clearly this cannot be known *a priori*. If we randomly choose the delay estimates from the potential values presented in Equations (20a)-(20c), this will result in poor performance. Thus we need to analyze the selection of m_1 and m_2. To this end, Proposition 1 provides this design guidance for the noiseless case.

Proposition 1: When the rectangular pulse shape is adopted for the signal model given in Equation (5), the uniqueness of the delay estimates can be guaranteed for the noiseless case ($e^{(r_k)} = 0$) with any $m_1, m_2 \in (0, M-1]$ and there is a closed-form expression for the delay estimate.

Proof: See Appendix A. □

Remark 1: Based on Proposition 1 and its proof, after the ratio function $f_R(t_k)$ is obtained, it is compared with two thresholds $\Gamma_1 = 1 + \frac{m_1 T_s - m_2 T_s}{T}$ and $\Gamma_2 = 1 + \frac{m_2 T_s - m_1 T_s}{T + m_1 T_s - m_2 T_s}$ to determine which equations (Equation (20a), (20b), or (20c)) we need to use as the delay estimate.

Then, we consider a perturbation $e^{(r_k)}$ to the noiseless ratio function $f_R(t_k)$, *i.e.*, $r_R(t_k) = f_R(t_k) + e^{(r_k)} = \frac{p(m_2 T_s - t_k)}{p(m_1 T_s - t_k)} + e^{(r_k)}$, where $0 \le m_1 < m_2 \le M-1$. Correspondingly, the error in the delay estimate is given by

$$e^{(t_k)}(m_1, m_2) = t_k - \hat{t}_k, \tag{21}$$

which is a function of m_1 and m_2. To reduce the error in the delay estimates, the design of m_1 and m_2 is analyzed in Lemma 1.

Lemma 1: For the rectangular pulse shape, $|e^{(t_k)}(m_1, m_2)|$ monotonically decreases as m_1 decreases or m_2 increases, if A) $\delta(k) > -1$ for $1 \le k \le p_0$.

Proof: See Appendix B. □

Remark 2: From Lemma 1, a smaller value of m_1 or a larger value of m_2 yields a greater reduction in delay estimate errors. Therefore, the best performance is achieved when $m_1 = 0$ and $m_2 = M-1$, which will be further discussed in Section V.

Remark 3: We observe that the monotonic relationship between m_i $(i = 1, 2)$ and the error appears to hold on average for $\delta(k) < -1$, but not for each realization.

B. Gaussian Pulse Shape

We next consider the Gaussian pulse shape and define $p(t)$ as,

$$p(t) = \frac{1}{\sqrt{2\pi}\sigma} e^{-\frac{t^2}{2\sigma^2}}, \tag{22}$$

where $\sqrt{2}\sigma$ is the pulse half-duration. For the noiseless case, the ratio function corresponding to Equation (14) is given by

$$f_G(t_k) = \frac{p(m_2 T_s - t_k)}{p(m_1 T_s - t_k)} = e^{\frac{(m_1^2 - m_2^2)T_s^2 + 2(m_2 - m_1) t_k T_s}{2\sigma^2}}. \tag{23}$$

It is straightforward to verify that $f_G(t_k)$ is a monotone function with respect to t_k. We can obtain the unique delay estimate of the kth path as

$$\begin{aligned} \hat{t}_k &= \frac{2\sigma^2 \ln f_G(t_k) + (m_2^2 - m_1^2)T_s^2}{2(m_2 - m_1)T_s} \\ &= \frac{(m_2 + m_1)T_s}{2} + \frac{\sigma^2 \ln f_G(t_k)}{(m_2 - m_1)T_s}. \end{aligned} \tag{24}$$

If the ratio function has an error $e^{(r_k)}$, namely, $r_G(t_k) = f_G(t_k) + e^{(r_k)} = \frac{p(m_2 T_s - t_k)}{p(m_1 T_s - t_k)} + e^{(r_k)}$, the corresponding error in the delay estimate is

$$\begin{aligned} e^{(t_k)}(m_1, m_2) &= t_k - \hat{t}_k \\ &= \frac{\sigma^2}{(m_2 - m_1)T_s} \ln\left(\frac{f_G(t_k)}{f_G(t_k) + e^{(r_k)}}\right) \\ &= \frac{\sigma^2}{(m_2 - m_1)T_s} \ln\left(\frac{1}{1 + \delta(r_k)}\right). \end{aligned} \tag{25}$$

Proposition 2: For the Gaussian pulse shape described in Equation (22), and a fixed perturbation level $\delta(k)$, $|e^{(t_k)}(m_1, m_2)|$ is monotonically decreasing with increasing value of $|m_2 - m_1|$.

Proof: From Equation (25), it is straightforward to verify $\frac{\partial |e^{(t_k)}(m_1, m_2)|}{\partial (m_2 - m_1)} < 0$[2] if the value of σ and $\delta(k)$ are given. □

Remark 4: In order to combat the effect of perturbations, for fixed values of m_i $(i = 1, 2)$, one should select the smallest possible σ as seen in Equation (25). This is intuitive, as a smaller σ translates to a larger bandwidth.

Remark 5: The perturbation analysis in Section V also shows that noise sensitivity is decreased with larger $m_2 - m_1$. Thus, we conclude that the best performance is achieved when $m_2 - m_1$ is maximized for the Gaussian pulse shape, which is when $m_2 - m_1 = M - 1$. These observations are validated in the numerical results (see Section V).

C. Root-Raised-Cosine Pulse Shape

Finally, we consdier the RRC pulse shape. As such $p(t)$ is defined as

$$p(t) = \begin{cases} \dfrac{\pi}{4T} \operatorname{sinc}\left(\dfrac{1}{2\beta}\right), & t = \pm\dfrac{T}{2\beta}; \\ \dfrac{1}{T} \operatorname{sinc}\left(\dfrac{t}{T}\right) \dfrac{\cos\left(\dfrac{\pi\beta t}{T}\right)}{1 - \left(\dfrac{2\beta t}{T}\right)^2}, & \text{otherwise}, \end{cases} \tag{26}$$

where $\operatorname{sinc}(t) = \frac{\sin(\pi t)}{\pi t}$, β and T are the roll-off factor and a design parameter of $p(t)$, respectively. Viewing the design parameters m_1 and m_2 as constants, we consider the following noiseless ratio function for delay estimation,

$$\begin{aligned} & f_{RRC}(t_k) \\ &= \frac{p(m_2 T_s - t_k)}{p(m_1 T_s - t_k)} \\ &= \frac{\operatorname{sinc}\left(\frac{m_2 T_s - t_k}{T}\right) \cos\left(\frac{\pi\beta(m_2 T_s - t_k)}{T}\right) \left(1 - \left(\frac{2\beta(m_1 T_s - t_k)}{T}\right)^2\right)}{\operatorname{sinc}\left(\frac{m_1 T_s - t_k}{T}\right) \cos\left(\frac{\pi\beta(m_1 T_s - t_k)}{T}\right) \left(1 - \left(\frac{2\beta(m_2 T_s - t_k)}{T}\right)^2\right)}, \end{aligned} \tag{27}$$

where we assume $p(m_1 T_s - t_k) \neq 0$.[3]

[2] In fact, $\frac{\partial |e^{(t_k)}(m_1, m_2)|}{\partial (m_2 - m_1)}$ does not exist because $m_2 - m_1 \in \mathbb{Z}$ and $|e^{(t_k)}(m_1, m_2)|$ is not a continuous function with respect to $m_2 - m_1$. However, we can judge whether $|e^{(t_k)}(m_1, m_2)|$ is monotonically decreased with the increasing value of $m_2 - m_1$ by exploring the monotonicity of $|e^{(t_k)}(m_1, m_2)|$ with $m_2 - m_1 \in \mathbb{R}$.

[3] If we have $p(m_1 T_s - t_k) = 0$ and $p(m_2 T_s - t_k) \neq 0$, the delay estimate of the kth path can be directly obtained.

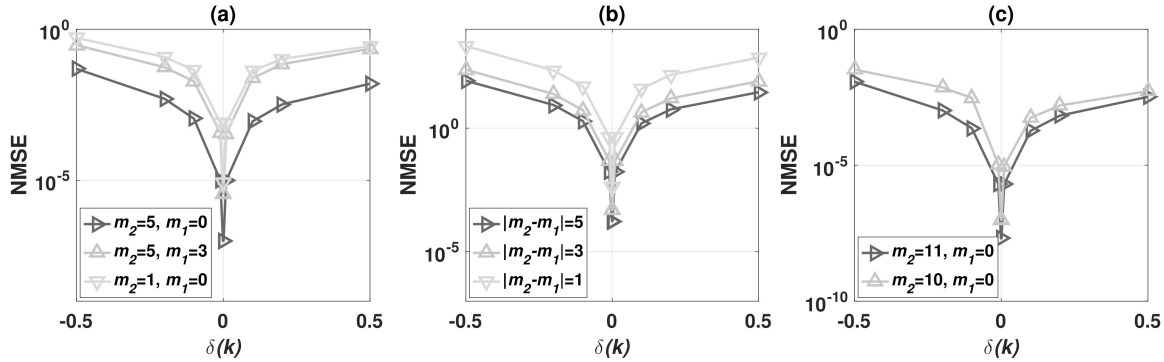

Fig. 1. NMSE of delay estimation under different fixed perturbation levels, (a) rectangular pulse shaping, (b) Gaussian pulse shaping, and (c) RRC pulse shaping.

In general, $f_{RRC}(t_k)$ is not a monotonic function with respect to t_k and thus the uniqueness of the delay estimate cannot be guaranteed. To make the delay estimate unique for the noiseless case, we need to properly select the design parameters m_i $(i = 1, 2)$, which is discussed in Proposition 3.

Proposition 3: For the RCC pulse shape, the uniqueness of the delay estimates in the noiseless case ($e^{(r_k)} = 0$) can be guaranteed and there is a closed-form expression for the delay estimate if:

C1) $m_1 = 0$ and $m_2 \in [\frac{2M}{1+\sqrt{2}}, M-1]$,[4] where m_1 and $m_2 \in \mathbb{Z}$;

C2) The parameters T and β in Equation (26) are such that $T = \beta m_2 T_s$ and $\frac{1}{\beta} \in \mathbb{Z}$.

Proof: See Appendix C. □

Remark 6: In contrast to the noiseless case, the conditions of Proposition 3 do not guarantee a unique estimate for all possible perturbations to the ratio function $e^{(r_k)}$. Each perturbation value yields a different optimal m_2 value within $[\frac{2M}{1+\sqrt{2}}, M-1]$. In practice, the perturbation is unknown. However, one can consider multiple values of m_2 and average the corresponding delay estimates.

In Section V, we will numerically examine the influence of the choice of m_2 on the accuracy of the delay estimation and further discuss the performance degradation caused by violation of the conditions in Proposition 3.

V. Simulation Results

In this section, we evaluate the performance of our proposed scheme. First, the effects of the perturbations on the delay estimation are numerically presented, with the rectangular, Gaussian, and RRC pulse shapes all explicitly considered, respectively. Then, our proposed scheme is compared with PLAN [16] to the show the two key performance improvements: lower BER with re-sampling and more accurate estimation with re-estimation.

A. Signal Parameters

The channel model is constructed based on Equation (2). Specifically, the delays are uniform random variables, normalized to $(0, 1]$ and the normalized Doppler shifts (also uniform random variables) have a support $[-\frac{1}{2}, \frac{1}{2}]$. The channel gains and noise are complex, independent, Gaussian random variables. The pilot sequence is a Binary Phase Shift Keying (BPSK) modulated random sequence, *i.e.*, $\{-1, +1\}$ with equal probability. As previously noted, the pulse shapes, $p_t(t) = p_r(t)$, are chosen as the rectangular, Gaussian, or RRC pulse shapes. Correspondingly, we set $p(t)$ based on Equations (18), (22), or (26), truncated by a window with length of $2MT_s$. For the optimization problem in Equations (10), we set ϵ to $\sigma_z\sqrt{N + 2\sqrt{N \log N}}$ [30] with σ_z^2 being the variance of $z[n]$, $1 \le n \le N$. In all of these experiments, the scaling law developed in [16] is satisfied to ensure proper behavior of the atomic norm based estimator and we set p_0 and T_s to 3, and $\frac{\tau_{\max}}{M} + \frac{1}{2}(\frac{\tau_{\max}}{M-1} - \frac{\tau_{\max}}{M})$, respectively. Unless otherwise stated, M is set to 6 and the SNR is defined as the transmit SNR averaged over the pilot and the data sequence. We make no assumptions on the modulation scheme and arbitrary values of p_0 can be accommodated assuming a sufficiently large value of N.

B. Perturbation Analysis

The influence of the perturbation on the errors in the delay estimates is further analyzed using simulations to back up theoretical analysis in Section IV. The NMSE of delay estimation under the fixed perturbation levels $\delta(k)$ is presented in Fig. 1, where N is set to 150 for the simulations of perturbation analysis. Furthermore, the NMSE performance under different SNRs is shown in Fig. 2 to statistically validate the analysis. We define the NMSE as $\text{NMSE} = \frac{\|\boldsymbol{\gamma} - \hat{\boldsymbol{\gamma}}\|_2^2}{\|\boldsymbol{\gamma}\|_2^2}$, where $\boldsymbol{\gamma}$ is the true value of the target parameter and $\hat{\boldsymbol{\gamma}}$ denotes its estimated value.

We first consider the rectangular pulse shape; the NMSE of the delay estimates is presented in Figs. 1(a) and 2(a), where T defined in Equation (18) is set to MT_s. Consistent with the analysis in Proposition 1, Figs. 1(a) and 2(a) show that a smaller value of m_1 or a larger value of m_2 can help decrease the error in the delay estimate, making it less sensitive to the perturbation, even though condition A of Lemma 1 is not always satisfied for a given SNR.

For the implementation of ANDE with the Gaussian pulse shape, we set σ to 1. The NMSE of delay estimation is shown

[4]Note that, the constraint $m_2 \in [\frac{2M}{1+\sqrt{2}}, M-1]$ enforces $M \ge 6$ because $m_2 \in \mathbb{Z}$ and $m_2 > m_1 = 0$ holds, which enables the consideration of large (*i.e.* $M \ge 6$) discrete delay spreads. The condition $M \ge 6$ can be met by decreasing the sampling period T_s.

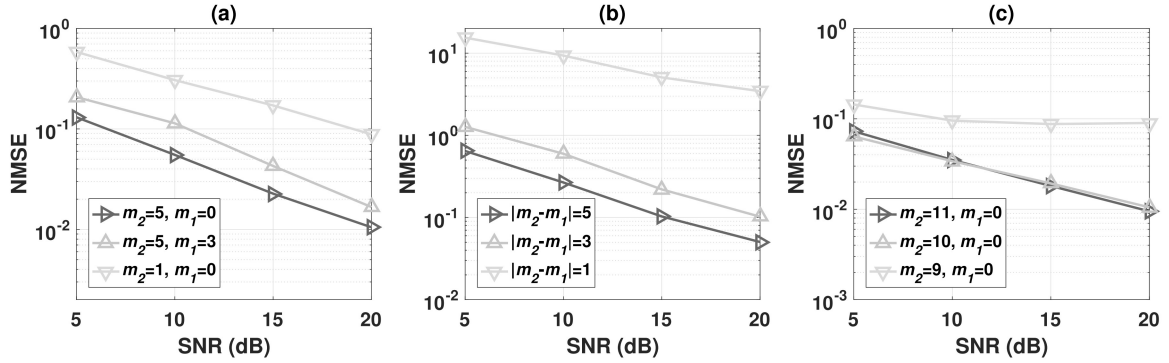

Fig. 2. NMSE of delay estimation under different SNRs, (a) rectangular pulse shaping, (b) Gaussian pulse shaping, and (c) RRC pulse shaping.

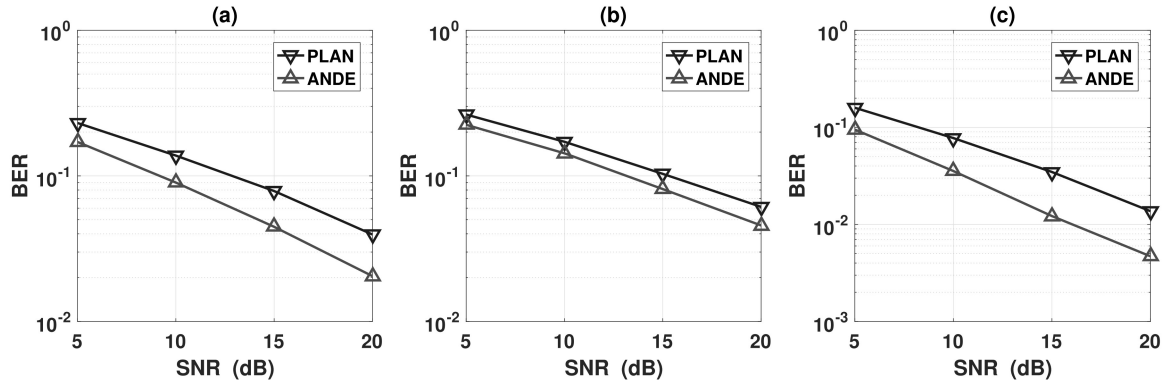

Fig. 3. BER of the data sequence under different SNRs, (a) rectangular pulse shaping, (b) Gaussian pulse shaping, and (c) RRC pulse shaping.

in Figs. 1(b) and 2(b). It can be observed that, for both the fixed perturbation level and the random perturbation, with the increasing value of $|m_2 - m_1|$, the NMSE of delay estimation is dramatically reduced. Furthermore, using a larger value of $|m_2 - m_1|$ causes the NMSE of delay estimation to increase more slowly as the perturbation level increases. Therefore, for the Gaussian pulse shape, we seek to maximize $|m_2 - m_1|$.

For the RRC pulse, Proposition 3 dictates $m_1 = 0$ and $m_2 \in [\frac{2M}{1+\sqrt{2}}, M-1]$. In Fig. 1(c), the NMSE of delay estimation using ANDE with RRC pulse shapes are plotted, where m_1, M, β and T in Equation (26) are set to 0, 12, $\frac{1}{2}$ and $m_2\beta T_s$, respectively. Based on Proposition 3, there are two choices of m_2 to ensure unique delay estimates, *i.e.*, $m_2 = 11$ or 10. From Fig. 1(c), for fixed perturbation levels, a relatively lower NMSE of delay estimation is achieved with a larger value of m_2, where the Doppler shift of each path is assumed to be perfectly estimated before the Algorithm 1 is implemented. Under different SNRs, a slightly lower NMSE of delay estimation is achieved with a smaller value of m_2 if the SNR is less than than 12dB, but a larger value of m_2 leads to the reduction of errors in the delay estimates as SNR increases. Consistent with our analysis, we see that there is no optimal design of m_2 for all perturbations.

To visualize the impact of the violation of conditions in Proposition 3, we set $m_1 = 0$ and $m_2 = 9$. To obtain the delay estimates of this case, we search for the potential value $\hat{t}_k$ in $(0, 1]$ for each path that minimizes $\|\frac{p(m_2T_s - \hat{t}_k)}{p(m_1T_s - \hat{t}_k)} - f_{RRC}(t_k)\|_2$. The associated NMSE for this case is also shown in Fig. 2(c). As uniqueness is not guaranteed, a strong performance loss is seen, as suggested by Proposition 3.

C. Bit Error Performance Comparison

We first consider the BER of our proposed method and compare to that of PLAN. The motivation behind considering BER first is that for the leakage vector and Doppler values the NMSE of ANDE is exactly that of PLAN, *i.e.* PLAN is used to initialize ANDE. However, we will consider the impact of re-sampling and re-estimation within ANDE and compare to PLAN in the sequel. We underscore that for BER computation, ANDE **does** re-sample the signal exploiting the estimates of all channel parameters.

To show the performance gains achieved by our scheme, the BER for data detection with ANDE and PLAN [16] are shown in Fig. 3, where N, m_1, m_2, M, σ, β, and the support of the rectangular pulse shape T are set to 64, 0, 5, 6, 1, $\frac{1}{2}$ and $2MT_s$. Maximum likelihood sequence equalization [31] is implemented for detection. Note that, these design parameters are selected based on the theoretical analysis in Section IV, which ensures the uniqueness of delay estimates for the noiseless ratio function and yields delay estimation that is relatively robust to noise. For each Monte Carlo, a sequence of 150 i.i.d. BPSK symbols is generated. The average BER for each sequence is determined and then averaged over each Monte Carlo run.

As shown in Fig. 3, ANDE outperforms PLAN, offering 2.5dB to 5dB improvement on average. This strong gain is

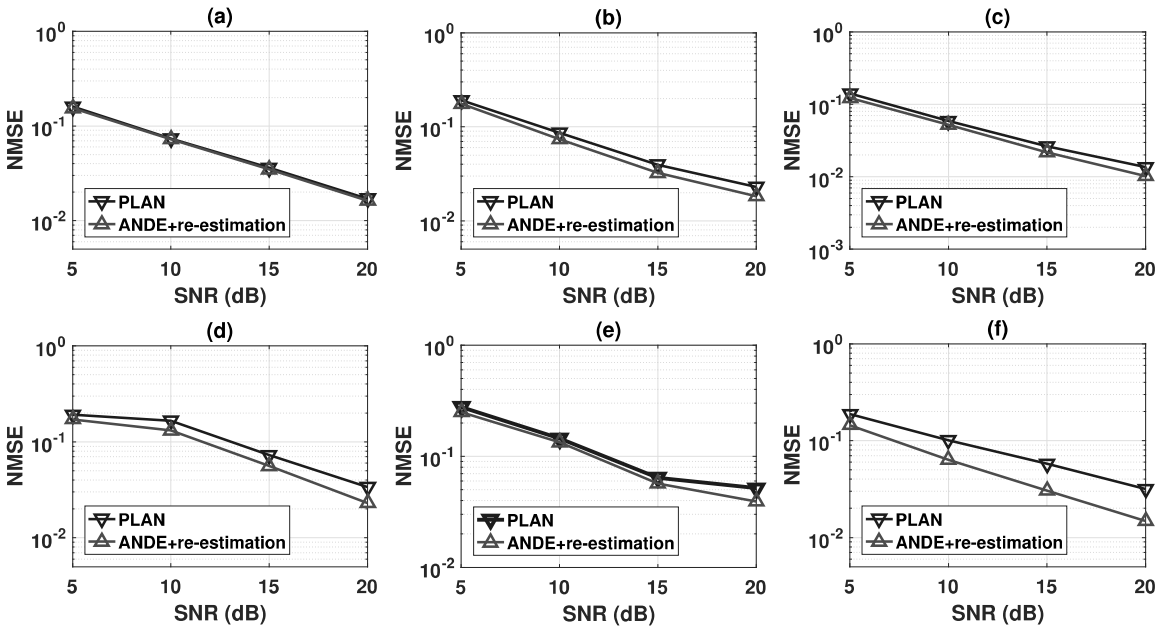

Fig. 4. NMSE of channel matrix estimation under different SNRs, (a) rectangular pulse shaping, (b) Gaussian pulse shaping, and (c) RRC pulse shaping; NMSE of Doppler shift estimation under different SNRs, (d) rectangular pulse shaping, (e) Gaussian pulse shaping, and (f) RRC pulse shaping.

achieved as the individual delays, Doppler values, and channel gains are estimated via ANDE enabling the construction of receive filtering based on the pulse shape and the channel; whereas PLAN only estimates the channel matrix described in Equations (7). Essentially, with channel parameters individually recovered using ANDE, properly re-sampling the received signal increases the signal-to-interference-plus-noise ratio on average, beneficial to the accurate signal detection.

D. Estimation Accuracy Performance Comparison

Since our purpose is to estimate the channel parameters and recover the transmitted signal as accurately as possible, we then numerically analyze the NMSE of the channel matrix and Doppler shifts estimation to show the performance improvements with our scheme. Since the estimates of delays and channel gains are not available via PLAN as explained in Section III-B, $t^{\star}(n)$ is set to 0. Nevertheless, these parameters can be separately estimated via ANDE and thus $t^{\star}(n)$ can be properly adjusted based on this complete channel side information. Finally, the re-sampled signals are used as the pilot sequence for re-estimation. We set $t^{\star}(n)$ to $\hat{t}_1$ in the following experiments.

Figures 4(a)-(c) show the NMSE of the channel matrix estimation using ANDE and PLAN, where all the design parameters of pulse shapes are the same as that in Section V-C. From Figs. 4(a)-(c), we can observe that, as compared with PLAN, lower NMSE of channel matrix estimation is achieved by re-estimation with the properly re-sampled signals, where individual channel parameters are estimated using ANDE, when the Gaussian pulse shape, the rectangular pulse shape or the RCC pulse shape is adopted during transmissions. In contrast to PLAN where the delays and channel gains are not explicitly estimated, with these parameters recovered via ANDE, re-sampling the received continuous-time signal equivalently reduces the delay spreads. This makes it easier to estimate the channel parameters, which is one reason for the performance improvements shown in Figs. 4(a)-(c). In comparing the NMSE plots to the BER plots, we see that modest improvements in NMSE via ANDE and re-estimation can often lead to larger gains with respect to the BER. This phenomenon was also observed in [27]. The key is that the improved estimation methods provide better estimates for the more critical channel parameters - those that impact BER performance.

In addition, the NMSE of Doppler shift estimation is plotted in Figs. 4(d)-(f), where implementing ANDE and re-estimation yields a more accurate Doppler shift estimation. There is an apparent 1dB to 5dB gain on average in the SNR sense as compared with PLAN.

VI. Conclusions

In this paper, an improvement to an atomic norm based estimation scheme is proposed for time-varying narrowband leaked channels, where all the channel parameters can be individually estimated. In particular, a new strategy to estimate delays and channel gains after atomic norm based channel matrix estimation [16] is provided. The analysis regarding the uniqueness of delay estimates in the presence of Gaussian pulse shapes, rectangular pulse shapes or RRC pulse shapes and the accompanying perturbation study for the noisy case are provided. Despite its simplicity, the new method offers strong improvement with respect to BER over the prior art (2.5dB to 5dB) [16]. Direct estimation of the delays is an essential element of high performance channel equalization, as well as localization strategies; thus the proposed methods have many practical applications. The proposed method can also be used to further improve channel matrix and Doppler estimation.

APPENDIX A
PROOF OF PROPOSITION1

Based on Equations (20a)-(20c), there are three potential delay estimates for each path. Since t_k is unknown, we cannot directly distinguish which estimate is the desired one. However, because $\frac{\partial f_R(t_k)}{\partial m_2} > 0$ always holds, the delay estimate is unique and can be obtained by comparing the ratio function with two fixed thresholds Γ_1 and Γ_2.

Recall that, in Section IV, it is assumed that $2T_s \ll T$ and $T \geq MT_s$ holds for the rectangular pulse shape. Given the presence of channel leakage, we have that $M \geq 2$ and $(M-1)T_s \leq \tau_{\max} < MT_s$, with the use of the definition of the maximum discrete delay spread. Therefore, it can be verified that $1 > f_R(t_k) > 0$ if $m_2T_s > m_1T_s \geq t_k > 0$, $f_R(t_k) > -1$ if $m_2T_s \geq t_k > m_1T_s$, and $f_R(t_k) > 1$ if $MT_s > t_k > m_2T_s > m_1T_s$.

For the noiseless case ($e^{(r_k)} = 0$), to ensure the uniqueness of the delay estimates, $\hat{t}_k = t_k$ needs to be enforced for a given $f_R(t_k)$. Therefore, $m_1T_s \geq \hat{t}_k > 0$, $m_2T_s \geq \hat{t}_k > m_1T_s$ and $MT_s > \hat{t}_k > m_2T_s$ hold for Equations (20a), (20b) and (20c), respectively. Specifically, suppose that $\hat{t}_k$ takes the estimate given in Equation (20a), we need to ensure

$$\hat{t}_k = m_1T_s - T + \frac{(m_1 - m_2)T_s}{f_R(t_k) - 1} \leq m_1T_s,$$

and equivalently we can obtain

$$f_R(t_k) \leq \Gamma_1,$$

where $\Gamma_1 = 1 + \frac{m_1T_s - m_2T_s}{T}$. If $\hat{t}_k$ takes the estimate presented in Equation (20b), the following condition needs to be met,

$$m_1T_s < \hat{t}_k = m_1T_s + T + \frac{(m_2 - m_1)T_s - 2T}{f_R(t_k) + 1} \leq m_2T_s,$$

and thus we have

$$\Gamma_1 < f_R(t_k) \leq \Gamma_2,$$

with $\Gamma_1 = 1 + \frac{m_2T_s - m_1T_s}{T + m_1T_s - m_2T_s}$. Similarly, if $t_k > m_2T_s$, it can verified that

$$\Gamma_2 < f_R(t_k).$$

Based on the above analysis, after we obtain $f_R(t_k)$, this ratio function is compared with Γ_1 and Γ_2, and the unique delay estimate can be rewritten as

$$\hat{t}_k = \begin{cases} m_1T_s - T + \dfrac{(m_1 - m_2)T_s}{f_R(t_k) - 1}, & \text{if } f_R(t_k) \leq \Gamma_1; \\ m_1T_s + T + \dfrac{(m_2 - m_1)T_s - 2T}{f_R(t_k) + 1}, & \text{if } \Gamma_1 < f_R(t_k) \leq \Gamma_2; \\ m_1T_s + T + \dfrac{(m_1 - m_2)T_s}{f_R(t_k) - 1}, & \text{otherwise.} \end{cases} \tag{28}$$

APPENDIX B
PROOF OF LEMMA 1

To prove Lemma 1, with the existence of the perturbation, we need to show $|e^{(t_k)}(m_1, m_2)|$ is monotonically decreasing with respect to m_1 while monotonically increasing with respect to m_2, for a fixed perturbation level $\delta(k)$.

Recall that, $T \geq MT_s$ is ensured for this kind of pulse shape and thus $T > \max\{m_2T_s, t_k\}$ holds. Furthermore, since $\delta(k)$ is assumed to be greater than -1 according to the condition A, we can derive $|e^{(t_k)}(m_1, m_2)|$ in Equation (29), as shown at the top of the next page, by substituting Equations (19) and (28) into Equation (21).

With some algebra, the first-order partial derivatives of $|e^{(t_k)}(m_1, m_2)|$ with respect to m_1 and m_2, *i.e.*, $\frac{\partial |e^{(t_k)}(m_1,m_2)|}{\partial m_1}$ and $\frac{\partial |e^{(t_k)}(m_1,m_2)|}{\partial m_2}$,[5] can be derived, respectively. With the conditions $T > \max\{m_2T_s, t_k\}$ and $\delta(k) > -1$, it can be verified that $\frac{\partial |e^{(t_k)}(m_1,m_2)|}{\partial m_1} > 0$ and $\frac{\partial |e^{(t_k)}(m_1,m_2)|}{\partial m_1} < 0$ hold. Therefore, $|e^{(t_k)}(m_1, m_2)|$ is monotonically decreasing with respect to m_1 while monotonically increasing with respect to m_2.

APPENDIX C
PROOF OF PROPOSITION 3

By designing $q_1 = \frac{T}{T_s}$, $q_2 = \frac{m_2}{q_1}$ and $q_3 = \frac{\beta m_2}{q_1}$, we have $q_1 > 1$, $m_2 > q_2 \geq 1$, $\beta m_2 > q_3 \geq 1$, $q_1 \in \mathbb{R}$, and $q_2, q_3 \in \mathbb{Z}$ since the condition $C2$ is assumed. When m_1 is set to 0 according to the assumption $C1$, the ratio function $f_k(t_k)$ can be rewritten as

$$f_{RRC}(t_k) = \frac{(-1)^{(q_2+q_3)} t_k (q_1T_s - 2\beta t_k)}{(q_1q_2T_s - t_k)\,(2\beta t_k - (2q_3 - 1)\,q_1T_s)} \times \frac{(q_1T_s + 2\beta t_k)}{(2\beta t_k - (2q_3 + 1)\,q_1T_s)}, \tag{31}$$

where $t_k \in (0, MT_s)$ and $t_k \neq \frac{1}{2q_3} m_2T_s$, $(1 - \frac{1}{2q_3})m_2T_s$, m_2T_s, or $(1 + \frac{1}{2q_3})m_2T_s$, for all k.

To ensure the uniqueness of the delay estimates, we need to analyze the monotonicity of $f_{RRC}(t_k)$. The first-order derivative of $f_{RRC}(t_k)$ with respect to t_k is given by

$$\frac{\partial f_{RRC}(t_k)}{\partial t_k} = \frac{(-1)^{q_2+q_3}(t_k - t_k^{(1)})(t_k - t_k^{(2)})(t_k - t_k^{(3)})(t_k - t_k^{(4)})}{\left((t_k - q_1q_2T_s)\,(q_1^2T_s^2 - 4\beta^2(t_k - q_1q_2T_s)^2)\right)^2}, \tag{32}$$

where

$$t_k^{(1)} = \frac{q_1q_2T_s}{2}\left(1 - \sqrt{1 + \frac{\sqrt{4q_3^2 - 1}}{\sqrt{3}q_3^2}}\right),$$

$$t_k^{(2)} = \frac{q_1q_2T_s}{2}\left(1 - \sqrt{1 - \frac{\sqrt{4q_3^2 - 1}}{\sqrt{3}q_3^2}}\right),$$

$$t_k^{(3)} = \frac{q_1q_2T_s}{2}\left(1 + \sqrt{1 - \frac{\sqrt{4q_3^2 - 1}}{\sqrt{3}q_3^2}}\right),$$

[5] $\frac{\partial |e^{(t_k)}(m_1,m_2)|}{\partial m_1}$ and $\frac{\partial |e^{(t_k)}(m_1,m_2)|}{\partial m_2}$ do not exist because $m_1, m_2 \in \mathbb{Z}$ and $|e^{(t_k)}(m_1, m_2)|$ is not a continuous function with respect to m_1 and m_2. However, we still can judge whether $|e^{(t_k)}(m_1, m_2)|$ is monotonic with respect to m_1 or m_2 by exploring the monotonicity of $|e^{(t_k)}(m_1, m_2)|$ with $m_1, m_2 \in \mathbb{R}$.

$$|e^{(t_k)}(m_1,m_2)| = \begin{cases} \dfrac{|\delta(k)|(T+t_k-m_2T_s)(T+t_k-m_1T_s)}{-\delta(k)(T+t_k-m_2T_s)+m_2T_s-m_1T_s}, & \text{if } f_R(t_k)\le\Gamma_1, t_k\le m_1T_s; \\ \dfrac{(T+t_k-m_2T_s)((2+\delta(k))(m_1T_s-t_k)+\delta(k)T)}{\delta(k)(T+t_k-m_2T_s)+2T+2t_k-m_2T_s-m_1T_s}, & \text{if } \Gamma_1<f_R(t_k)\le\Gamma_2, t_k\le m_1T_s; \\ \dfrac{\delta(k)(T+t_k-m_2T_s)(T-t_k+m_1T_s)-2T(m_2T_s-m_1T_S)}{\delta(k)(T+t_k-m_2T_s)-m_2T_s+m_1T_s}, & \text{if } \Gamma_2<f_R(t_k), t_k\le m_1T_s; \\ \dfrac{(T+t_k-m_2T_s)(\delta(k)(T+t_k-m_1T_s)+2t_k-2m_1T_s)}{\delta(k)(T+t_k-m_2T_s)+2t_k-m_2T_s-m_1T_s}, & \text{if } f_R(t_k)\le\Gamma_1, m_1T_s<t_k\le m_2T_s; \\ \dfrac{|\delta(k)|(T-t_k+m_1T_s)(\delta(k)(T+t_k-m_2T_s)+2t_k-2m_2T_s)}{\delta(k)(T+t_k-m_2T_s)+2t_k-m_1T_s-m_2T_s}, & \text{if } \Gamma_2<f_R(t_k), m_1T_s<t_k\le m_2T_s; \\ \dfrac{\delta(k)(T+t_k-m_1T_s)(T-t_k+m_2T_s)+2T(m_2T_s-m_1T_s)}{\delta(k)(T-t_k+m_2T_s)+m_2T_s-m_1T_s}, & \text{if } f_R(t_k)\le\Gamma_1, m_2T_s<t_k; \\ \dfrac{-(T-t_k+m_1T_s)(\delta(k)(T-t_k+m_2T_s)-2t_k+2m_2T_s)}{\delta(k)(T-t_k+m_2T_s)+2T-2t_k+m_2T_s+m_1T_s}, & \text{if } \Gamma_1<f_R(t_k)\le\Gamma_2, m_2T_s<t_k; \\ \dfrac{|\delta(k)|(T-t_k+m_1T_s)(T-t_k+m_2T_s)}{\delta(k)(T-t_k+m_2T_s)+m_2T_s-m_1T_s}, & \text{if } \Gamma_2<f_R(t_k), m_2T_s<t_k; \\ \dfrac{|\delta(k)|(T+t_k-m_2T_s)(T-t_k+m_1T_s)}{\delta(k)(T+t_k-m_2T_s)+2T+m_1T_s-m_2T_s}, & \text{otherwise.} \end{cases} \tag{29}$$

$$\hat{t}_k = \begin{cases} \dfrac{\left(5f_{RRC}(t_k)+\sqrt{f_{RRC}^2(t_k)-(-1)^{\frac{1}{\beta}}34f_{RRC}(t_k)+1}-(-1)^{\frac{1}{\beta}}\right)m_2T_s}{4(f_{RRC}(t_k)+(-1)^{\frac{1}{\beta}})}, & \text{if } f_{RRC}(t_k)<0; \\ \dfrac{m_2T_s}{2}, & \text{if } f_{RRC}(t_k)=(-1)^{\frac{1}{\beta}+1}; \\ \dfrac{\left(5f_{RRC}(t_k)-\sqrt{f_{RRC}^2(t_k)-(-1)^{\frac{1}{\beta}}34f_{RRC}(t_k)+1}-(-1)^{\frac{1}{\beta}}\right)m_2T_s}{4(f_{RRC}(t_k)+(-1)^{\frac{1}{\beta}})}, & \text{otherwise} \end{cases} \tag{30}$$

and

$$t_k^{(4)} = \frac{q_1q_2T_s}{2}\left(1+\sqrt{1+\frac{\sqrt{4q_3^2-1}}{\sqrt{3}q_3^2}}\right).$$

It can be verified that

$$t_k^{(1)} \le 0 \le t_k^{(2)} \le \frac{m_2T_s}{2} \le t_k^{(3)} \le m_2T_s \le t_k^{(4)}.$$

Therefore, if $t_k^{(2)} \neq t_k^{(3)}$, the ratio function $f_{RRC}(t_k)$ is not monotonic with respect to t_k when $t_k \in (0, MT_s)$ and multiple delay estimates may exist for a given $f_{RRC}(t_k)$. However, since the assumptions $C1$ and $C2$ hold, we have $q_3 = 1$ and the following two conditions are satisfied,

1) $t_k^{(2)} = t_k^{(3)}$,
2) $t_k^{(4)} \ge MT_s$.

With the above two conditions, the ratio function in Equation (31) can be simplified into

$$f_{RRC}(t_k) = \frac{(-1)^{q_2}t_k(q_1T_s+2\beta t_k)}{(q_1q_2T_s-t_k)(2\beta t_k-3q_1T_s)}. \tag{33}$$

Then, we can derive that when $t_k \in (0, m_2T_s)$ or $t_k \in (m_2T_s, MT_s)$, the following inequality holds

$$(-1)^{q_2}\frac{\partial f_{RRC}(t_k)}{\partial t_k} < 0,$$

proving $f_{RRC}(t_k)$ is a monotone function with respect to t_k. Also, we have

$$f_{RRC}(t')f_{RRC}(t'') < 0,$$

if $t' \in (0, m_2T_s)$ and $t'' \in (m_2T_s, MT_s)$. Therefore, given $f_{RRC}(t_k)$, the delay of all paths can be uniquely estimated.

By computing the inverse function of $f_{RRC}(t_k)$ given in Equation (33), the potential values of delay estimates are $\dfrac{\left(5\ f_{RRC}(t_k)+\sqrt{f_{RRC}^2(t_k)-(-1)^{\frac{1}{\beta}}34\ f_{RRC}(t_k)+1}-(-1)^{\frac{1}{\beta}}\right)m_2T_s}{4\left(f_{RRC}(t_k)+(-1)^{\frac{1}{\beta}}\right)}$ and $\dfrac{\left(5\ f_{RRC}(t_k)-\sqrt{f_{RRC}^2(t_k)-(-1)^{\frac{1}{\beta}}34\ f_{RRC}(t_k)+1}-(-1)^{\frac{1}{\beta}}\right)m_2T_s}{4\left(f_{RRC}(t_k)+(-1)^{\frac{1}{\beta}}\right)}$, with $f_{RRC}(t_k) \neq (-1)^{\frac{1}{\beta}+1}$.[6] Herein, it can be verified that $f_{RRC}^2(t_k) - (-1)^{\frac{1}{\beta}}34\ f_{RRC}(t_k) + 1 \ge 0$ holds for all $t_k \in (0, MT_s)$. Since the uniqueness of the delay estimate is ensured according to the above analysis, the remaining step is to discuss which potential value is the unique estimate for several cases, *i.e.*, a) $\frac{1}{\beta}$ is even and $f_{RRC}(t_k) > 0$; b) $\frac{1}{\beta}$ is even and $-1 < f_{RRC}(t_k) < 0$; c) $\frac{1}{\beta}$ is even and $f_{RRC}(t_k) < -1$; d) $\frac{1}{\beta}$ is odd and $f_{RRC}(t_k) < 0$; e) $\frac{1}{\beta}$ is odd and $0 < f_{RRC}(t_k) < 1$; f) $\frac{1}{\beta}$ is odd and $f_{RRC}(t_k) > 1$. By exploiting the properties of $f_{RRC}(t_k)$, we can determine the desired estimate with some algebra and the closed-form expression for the delay estimate is given in Equation (30), as shown at the top of the page.

[6] If $f_{RRC}(t_k) = (-1)^{\frac{1}{\beta}+1}$, it is straightforward to verify that $\hat{t}_k = \frac{m_2T_s}{2}$.

REFERENCES

[1] J. Li and U. Mitra, "Improved atomic norm based channel estimation for time-varying narrowband leaked channels," in *Proc. IEEE Int. Conf. Acoust., Speech Signal Process. (ICASSP)*, Jun. 2021, pp. 4825–4829.

[2] J. Wu and P. Fan, "A survey on high mobility wireless communications: Challenges, opportunities and solutions," *IEEE Access*, vol. 4, pp. 450–476, 2016.

[3] B. Gong, L. Gui, S. Luo, Y. L. Guan, Z. Liu, and P. Fan, "Block pilot based channel estimation and high-accuracy signal detection for GSM-OFDM systems on high-speed railways," *IEEE Trans. Veh. Technol.*, vol. 67, no. 12, pp. 11525–11536, Dec. 2018.

[4] S. Beygi, U. Mitra, and E. G. Ström, "Nested sparse approximation: Structured estimation of V2V channels using geometry-based stochastic channel model," *IEEE Trans. Signal Process.*, vol. 63, no. 18, pp. 4940–4955, Sep. 2015.

[5] L. Yang, L. Yang, and K. C. Ho, "Moving target localization in multistatic sonar using time delays, Doppler shifts and arrival angles," in *Proc. IEEE Int. Conf. Acoust., Speech Signal Process. (ICASSP)*, New Orleans, LA, USA, Mar. 2017, pp. 3399–3403.

[6] R. Essaadali and A. Kouki, "A new simple unmanned aerial vehicle Doppler effect RF reducing technique," in *Proc. IEEE Mil. Commun. Conf. (MILCOM)*, Baltimore, MD, USA, Nov. 2016, pp. 1179–1183.

[7] Y. Liu, Z. Tan, H. Hu, L. J. Cimini, and G. Y. Li, "Channel estimation for OFDM," *IEEE Commun. Surveys Tuts.*, vol. 16, no. 4, pp. 1891–1908, 4th Quart., 2014.

[8] Y. Li, L. J. Cimini, and N. R. Sollenberger, "Robust channel estimation for OFDM systems with rapid dispersive fading channels," *IEEE Trans. Commun.*, vol. 46, no. 7, pp. 902–915, Jul. 1998.

[9] S. F. Cotter and B. D. Rao, "Sparse channel estimation via matching pursuit with application to equalization," *IEEE Trans. Commun.*, vol. 50, no. 3, pp. 374–377, Mar. 2002.

[10] E. Aktas and U. Mitra, "Single-user sparse channel acquisition in multiuser DS-CDMA systems," *IEEE Trans. Commun.*, vol. 51, no. 4, pp. 682–693, Apr. 2003.

[11] M. Sharp and A. Scaglione, "Application of sparse signal recovery to pilot-assisted channel estimation," in *Proc. IEEE Int. Conf. Acoust., Speech Signal Process. (ICASSP)*, Las Vegas, NV, USA, Mar. 2008, pp. 3469–3472.

[12] G. Taubock, F. Hlawatsch, D. Eiwen, and H. Rauhut, "Compressive estimation of doubly selective channels in multicarrier systems: Leakage effects and sparsity-enhancing processing," *IEEE J. Sel. Topics Signal Process.*, vol. 4, no. 2, pp. 255–271, Apr. 2010.

[13] D. Eiwen, G. Taubock, F. Hlawatsch, H. Rauhut, and N. Czink, "Multichannel-compressive estimation of doubly selective channels in MIMO-OFDM systems: Exploiting and enhancing joint sparsity," in *Proc. IEEE Int. Conf. Acoust., Speech Signal Process. (ICASSP)*, Dallas, TX, USA, Mar. 2010, pp. 3082–3085.

[14] X. Liu, K. Anand, Y. L. Guan, L. Deng, P. Fan, and Z. Zhou, "BEM-PSP for single-carrier and SC-FDMA communication over a doubly selective fading channel," *IEEE Trans. Wireless Commun.*, vol. 19, no. 6, pp. 3924–3937, Jun. 2020.

[15] K. Anand *et al.*, "Pilot design for BEM-based channel estimation in doubly selective channel," *IEEE Trans. Veh. Technol.*, vol. 69, no. 2, pp. 1679–1694, Feb. 2020.

[16] S. Beygi, A. Elnakeeb, S. Choudhary, and U. Mitra, "Bilinear matrix factorization methods for time-varying narrowband channel estimation: Exploiting sparsity and rank," *IEEE Trans. Signal Process.*, vol. 66, no. 22, pp. 6062–6075, Nov. 2018.

[17] G. Tang, B. N. Bhaskar, P. Shah, and B. Recht, "Compressed sensing off the grid," *IEEE Trans. Inf. Theory*, vol. 59, no. 11, pp. 7465–7490, Nov. 2013.

[18] Y. Chi, "Joint sparsity recovery for spectral compressed sensing," in *Proc. IEEE Int. Conf. Acoust., Speech Signal Process. (ICASSP)*, Florence, Italy, May 2014, pp. 3938–3942.

[19] Y. Chi, "Guaranteed blind sparse spikes deconvolution via lifting and convex optimization," *IEEE J. Sel. Topics Signal Process.*, vol. 10, no. 4, pp. 782–794, Jun. 2016.

[20] A. Elnakeeb and U. Mitra, "Sparsity and rank exploitation for time-varying narrowband leaked OFDM channel estimation," in *Proc. IEEE Int. Conf. Acoust., Speech Signal Process. (ICASSP)*, Calgary, AB, Canada, Apr. 2018, pp. 3894–3898.

[21] A. Elnakeeb and U. Mitra, "On the Cramér–Rao bound of time-varying narrowband leaked MIMO OFDM channels," in *Proc. IEEE 19th Int. Workshop Signal Process. Adv. Wireless Commun. (SPAWC)*, Kalamata, Greece, Jun. 2018, pp. 1–5.

[22] A. Elnakeeb and U. Mitra, "On training sequence optimization for leaked MIMO OFDM channels," in *Proc. IEEE Global Commun. Conf. (GLOBECOM)*, Waikoloa, HI, USA, Dec. 2019, pp. 1–6.

[23] K. C. Ho, X. Lu, and L. Kovavisaruch, "Source localization using TDOA and FDOA measurements in the presence of receiver location errors: Analysis and solution," *IEEE Trans. Signal Process.*, vol. 55, no. 2, pp. 684–696, Feb. 2007.

[24] G. Wang, W. Zhu, and N. Ansari, "Robust TDOA-based localization for IoT via joint source position and NLOS error estimation," *IEEE Internet Things J.*, vol. 6, no. 5, pp. 8529–8541, Oct. 2019.

[25] Y. Han, Y. Shen, X.-P. Zhang, M. Z. Win, and H. Meng, "Performance limits and geometric properties of array localization," *IEEE Trans. Inf. Theory*, vol. 62, no. 2, pp. 1054–1075, Feb. 2016.

[26] S. Tomic, M. Beko, and R. Dinis, "RSS-based localization in wireless sensor networks using convex relaxation: Noncooperative and cooperative schemes," *IEEE Trans. Veh. Technol.*, vol. 64, no. 5, pp. 2037–2050, May 2015.

[27] N. Michelusi, U. Mitra, A. F. Molisch, and M. Zorzi, "UWB sparse/diffuse channels, Part I: Channel models and Bayesian estimators," *IEEE Trans. Signal Process.*, vol. 60, no. 10, pp. 5307–5319, Oct. 2012.

[28] M. Grant and S. Boyd. (2014). *CVX: MATLAB Software for Disciplined Convex Programming, Version 2.1*. [Online]. Available: http://cvxr.com/cvx

[29] B. Friedlander, "An efficient parametric technique for Doppler-delay estimation," *IEEE Trans. Signal Process.*, vol. 60, no. 8, pp. 3953–3963, Aug. 2012.

[30] T. T. Cai and L. Wang, "Orthogonal matching pursuit for sparse signal recovery with noise," *IEEE Trans. Inf. Theory*, vol. 57, no. 7, pp. 4680–4688, Jul. 2011.

[31] A. F. Molisch, *Wireless Communications*, vol. 34. Hoboken, NJ, USA: Wiley, 2012.

Jianxiu Li (Graduate Student Member, IEEE) received the B.S. degree in telecommunications engineering from Xidian University, Xi'an, China, in 2019. He is currently pursuing the Ph.D. degree with the Ming Hsieh Department of Electrical and Computer Engineering, University of Southern California, Los Angeles, CA, USA. His research interests include structured signal processing, channel estimation, and indoor localization.

Urbashi Mitra (Fellow, IEEE) received the B.S. and the M.S. degrees from the University of California at Berkeley and the Ph.D. degree from Princeton University. In Fall 2002, she was the Texas Instruments Visiting Professor with Rice University. She is currently the Gordon S. Marshall Professor in electrical engineering and computer science engineering with the University of Southern California. Her research interests include wireless communications, communication and sensor networks, biological communication systems, detection and estimation, and the interface of communication, sensing and control. She was a member of the IEEE Information Theory Society's Board of Governors from 2002 to 2007 and from 2012 to 2017, the IEEE Signal Processing Society's Technical Committee on Signal Processing for Communications and Networks from 2012 to 2017, the IEEE Signal Processing Society's Awards Board from 2017 to 2018, and the Chair/Vice Chair of the IEEE Communications Society's Communication Theory Technical Committee from 2017 to 2020. She was a recipient of the USC Viterbi Senior Research Award in 2021, the IEEE Communications Society Women in Communications Engineering Technical Achievement Award in 2017, the U.K. Royal Academy of Engineering Distinguished Visiting Professorship in 2016, the U.S. Fulbright Scholar Award in 2016, the U.K. Leverhulme Trust Visiting Professorship from 2016 to 2017, the Globecom Signal Processing for Communications Symposium Best Paper Award in 2012, the U.S. National Academy of Engineering Lillian Gilbreth Lectureship in 2012, the DCOSS Applications and Systems Best Paper Award in 2009, the Okawa Foundation Award in 2001, the OSU College of Engineering Lumley Award for Research in 2000, the OSU College of Engineering MacQuigg Award for Teaching in 1997, and the National Science Foundation CAREER Award in 1996. She was the inaugural Editor-in-Chief of IEEE TRANSACTIONS ON MOLECULAR, BIOLOGICAL AND MULTI-SCALE COMMUNICATIONS. From 2015 to 2016, she was a Distinguished Lecturer of the IEEE Communications Society.